Article

Fabrication of Novel Bio-Composites Based on Rice Milk for the Delivery of Capsaicinoids as Green Herbicides against *Cynodon dactylon* Weed

Gianluca Viscusi [1,*] **, Elena Lamberti** [1] **, Giovanna Aquino** [2] **, Manuela Rodriquez** [2] **and Giuliana Gorrasi** [1]

1   Department of Industrial Engineering, University of Salerno, Via Giovanni Paolo II, 132,
    84084 Fisciano, SA, Italy; ellamberti@unisa.it (E.L.); ggorrasi@unisa.it (G.G.)
2   Department of Pharmacy, University of Salerno, Via Giovanni Paolo II, 132, 84084 Fisciano, SA, Italy;
    gaquino@unisa.it (G.A.); mrodriquez@unisa.it (M.R.)
*   Correspondence: gviscusi@unisa.it

Abstract: In this paper, rice milk-based beads were fabricated through gelation in a calcium chloride solution. Green extraction of chili pepper in water/ethanol was conducted in order to obtain powder extract (PE) rich in apigenin C-pentosyl-C-hexoside, capsaicin, and dihydrocapsaicin. The effect of capsaicinoids loading on beads' properties was evaluated in terms of morphological and physical properties. Swelling phenomena and diameter variation of beads were studied as a function of time proving correspondence with the PE amount. The effect of ionic strength on bead swelling was considered. Kinetic studies of PE release were conducted to investigate the release profiles, which were modeled through a modified Baker and Lonsdale model by considering the change in mean diameter over time. The effect of PE loading was then correlated to the growth of *Cynodon dactylon* weed through in vivo tests. The results corroborate the performances of the encapsulated PE to be used as natural and green herbicide release systems able to inhibit the growth and the proliferation of weeds.

1. Introduction

The control of weeds and pests has been carried out by using traditional chemical pesticides in order to protect plants and crops and increase agricultural productivity. However, chemical pesticides are usually toxic since their enrichment in crops. The potential runoff and leaching of pesticides through the soil is currently a critical issue. Thus, the need of searching for botanical pesticides based on natural substances as an alternative to synthetic pesticides [1]. Since the long-lasting persistence of pesticides, they have been found in surface water, groundwater and even drinking water [2]. Moreover, they become easier to enter the food chain since their bioaccumulation properties [3–5]. All these dreadful considerations lead to the need for a green and innovative alternative to protect crops without leading to harmful consequences on the ecosystem [6,7]. A possible solution lies in the use of naturally derived substances [8] which could act as insecticides, antifeedants, insect-growth regulators, and repellents. Thus, the use of new approaches is highly recommended aiming of guaranteeing a controlled dispersion of green herbicides in soil. Controlled release methodologies have been studied as alternatives to avoid or reduce such problems [9]. Encapsulation is taking a central stage as a technique to design a controlled release device. Usually, an active compound is encapsulated in a biopolymer matrix, which acts as a slow or safe release carrier. Biodegradable polymeric matrices such as cellulose, agarose, starch, chitosan, gelatin or albumin are commonly employed [10–13]. In this work, rice milk was used as a matrix and sodium alginate was applied as gelling agent. The rice milk, which can be considered a grain milk made by processing rice, has

an average chemical composition based on protein (0.6%), carbohydrate (10.6%), sugar (4.0%), and fat (1.0%) [14]. Moreover, rice milk is rich in vitamins (thiamine, niacin, folate, riboflavin, etc.) as well as minerals; especially calcium, phosphorous, sodium, and magnesium [15]. Capsaicin (8-methyl-N-vanillyl-trans-6-nonenamide) is an active component of the extract of red chili pepper, used as food coloring and flavoring agents [10], exerting analgesic, anti-inflammatory and antibacterial activities [16]. More importantly, it possesses strong anti-microbial effects against gram-negative together with gram-positive bacteria and fungi [11,17]. Capsaicin, dihydrocapsaicin, nordihydrocapsaicin, homocapsaicin, and homodihydrocapsaicin are the five natural capsaicinoids. Among these, capsaicin and dihydrocapsaicin are the most predominant and biologically active ones [18]. According to the U.S. Environmental Protection Agency (U.S. EPA) chili pepper extract, thanks to its natural occurrence, can be classified as a biochemical pesticide. Since that, capsaicinoids were extracted from chili pepper using an environmentally friendly methodology. The polymer droplet gelation was finally applied as a green approach to design a soil-compatible polymeric matrix [19–21]. Based on the above, this research concerns the design and preparation of the green beads composite made up of rice milk, alginate, and capsaicinoids as a novel delivery system of green herbicides against a targeted weed (*Cynodon dactylon*). The obtained results will show the potentiality of the fabricated novel biocomposites as release devices of green herbicides to slow down and inhibit the proliferation of weeds. To the best of the authors' knowledge, there have been no scientific studies on the formulated biocomposites up to now.

2. Materials and Methods

2.1. Materials

Rice milk (Stammi Bene) was purchased from a local market. Sodium Alginate (CAS: 9005-38-3) was purchased from Sigma Aldrich. Calcium chloride (CAS: 10043-52-4) was purchased from Sigma Aldrich. Chili pepper, in powder form, was purchased from a local grocery. *Cynodon dactylon* seeds and soil were purchased from a local market.

2.2. Chili Pepper Extraction

Prior to produced rice milk beads, 10 g of chili pepper powder was solubilized in 150 mL of water/ethanol solution (50:50 *v/v*) for 24 h at 50 °C. Then, the mixture was filtered through a vacuum pump using a Whatman filter n.1. The chili pepper extract (PE) was dried at room temperature for 4 days.

2.3. Beads Preparation

Rice milk (10 g) and alginate (0.27 g) were mixed and stirred at 100 °C for 2 h. Chili pepper extract was added to the solution at different concentrations (0%, 2.5%, 10%, 20%). The solution was added dropwise to a 1.5% wt $CaCl_2$ solution to obtain beads. In order to achieve complete gelation, the beads were kept at 4 °C for 24 h. Next, they were recovered from the $CaCl_2$ solution and were washed with distilled water to fabricate the B-PE-x (x = % wt of PE into the composite beads). Finally, the produced beads were air dried for 72 h. Pure rice milk/alginate beads were fabricated in the same way. Figure 1 reports a schematization of the gelation process and, by way of example, the picture of B-PE-20%.
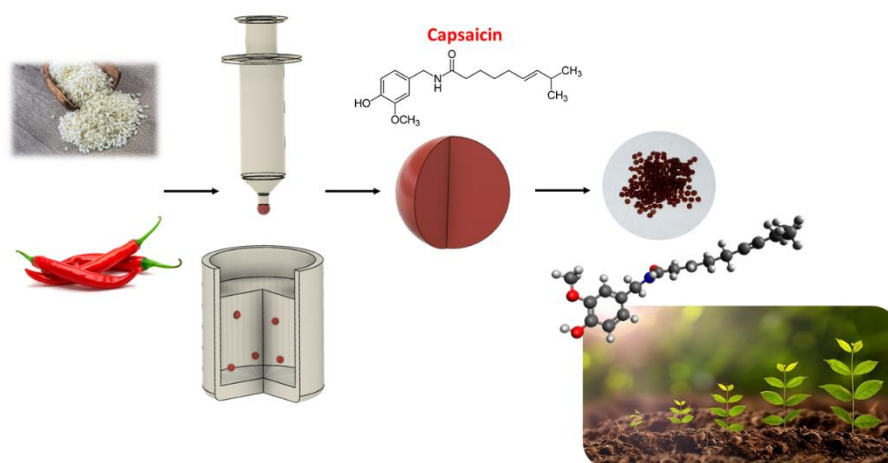
Figure 1. Schematization of gelation process of B-PE.

2.4. Methods

SEM analysis was conducted to investigate the morphology of beads. Before the analysis, samples were covered with a thin film of gold by sputtering. Images were acquired by a Phenom ProX microscope, working in high-vacuum mode.

The diameter of the beads was evaluated by analyzing digital images. Twenty beads were analyzed for each condition. The beads' diameters were obtained from recorded photographs and are expressed as the mean ± standard deviation.

The powder extract was solubilized in EtOH/H_2O (1:1% v/v) at a final concentration of 10 mg/mL and was subjected to a 0.45 μm membrane filter and directly injected into an HPLC system (Varian Medical Systems, Inc., Agilent, Santa Clara, CA, USA), consisting of a Varian 9012 binary solvent delivery unit, a Varian 9050 UV/Vis detector. HPLC analysis of the *C. annuum* extract was conducted on Luna® 5 μm C18(2) 250 × 4.6 mm (100 Å), packed with 5 μm core-shell particles column (Phenomenex, Bologna, Italy). The injection volume was 20 μL, and the flow rate was 1.0 mL min^{-1}.

Chromatograms were monitored at 280 nm at maximum absorbance of the compounds of interest. The mobile phase consisted of H_2O (A) and ACN (B), both acidified by formic acid 0.1% v/v. The analysis was performed in gradient elution as follows: 0.01–3.00 min, isocratic to 1% B; 3.01–21.00 min, 1–80% B; 21.01–25.00 min, isocratic to 80% B; and then five minutes for column re-equilibration. UHPLC-HRMS/MS analysis was performed on a Thermo Ultimate RS 3000 coupled online to a Q-Exactive hybrid quadrupole Orbitrap mass spectrometer (Thermo Fisher Scientific, Bremen, Germany) equipped with a heated electrospray ionization probe (HESI II). The separation was performed in reversed-phase mode, with a Kinetex® EVO C18 (150 × 2.1 mm; 2.6 m, 100) (Phenomenex, Bologna, Italy). The column temperature was set at 40 °C, and the flow rate was 0.3 mL/min. The mobile phase was (A): H_2O with 0.1% HCOOH (v/v) and (B): ACN with 0.1% HCOOH (v/v). The following gradient was employed: 0.01–3.00 min, isocratic to 1% B; 3.01–21.00 min, 1–80% B; 21.01–25.00 min, isocratic to 80% B; and then five minutes for column re-equilibration. Three μL were injected. All additives and mobile phases were LCMS grade and purchased from Merck (Milan, Italy).

The ESI was operated in positive (ESI+) and negative (ESI-) modes. The MS was calibrated by Thermo Calmix Pierce™ calibration solutions in both polarities. Full MS (150–1500 m/z) and data-dependent MS/MS were performed at a resolution of 35,000 and 17,500 FWHM respectively, normalized collision energy (NCE) values of 15, 20, and 25 were used. Source parameters: Sheath gas pressure, 50 arbitrary units; auxiliary gas flow, 13 arbitrary units; spray voltage, +3.5 kV, −2.8 kV; capillary temperature, 310 °C; auxiliary gas heater temperature, 300 °C. Data analysis and processing were performed using Xcalibur software v. 3.0.63 (Xcalibur Thermo Fischer Scientific, Waltham, MA, USA). The identification was based on standard retention time, accurate mass measurement,

elemental composition assignment, and MS/MS spectrum interpretation (Figure S1). The identification of capsaicin (*m/z* 306.2061), dihydrocapsaicin (*m/z* 308.2216), and apigenin-C-pentosyl-C-hexoside (*m/z* 563.1400) was achieved by comparison of their fragmentation pattern and the retention times previously reported in the literature [22].

Barrier properties to water vapor were evaluated using a DVS automated multi-vapor gravimetric sorption analyzer, using dry nitrogen as a carrier gas. Samples were exposed to increasing water vapor pressures obtaining different water activities $a_w = P/P_0$ (from $a_w = 0.1$ to $a_w = 0.8$), where P_0 is the saturation water pressure at the experimental temperature (30 °C). The adsorbed water mass was measured by a microbalance and recorded as a function of time; the equilibrium value of sorbed vapor, C_{eq} ($g_{solvent}/g_{dry\ basis}$) was evaluated. In order to analyze the sorption isotherms, different models were adopted: a polynomial model (Equation (1)), Langmuir isotherm [23] (Equation (2)), Freundlich isotherm [24] (Equation (3)) and Temkin isotherm [25] (Equation (4)):

$$q_e = A_0 + A_1 \times a_w + A_2 \times a_w{}^2 + A_3 \times a_w{}^3 + A_4 \times a_w{}^4 \tag{1}$$

$$q_e = \frac{q_m K_L c_e}{1 + K_L c_e} \tag{2}$$

$$q_e = K_F c_e{}^{1/n} \tag{3}$$

$$q_e = \frac{RT}{b} \ln(K_t c_e) \tag{4}$$

where q_e is the is the amount of the adsorbate at equilibrium (mg/g), A_i are constants of the polynomial model to be determined, c_e is the concentration of water (mg/L), q_m is the maximum adsorption capacity (mg/g), K_L is the Langmuir constant related to the energy of adsorption (L/mg), K_F is Freundlich constants (mg/g) (L/mg)$^{1/n}$, n is adsorption intensity, K_t is the equilibrium binding constant (L/mg) corresponding to the maximum binding energy, and the ratio RT/b is related to the heat of adsorption.

Swelling properties were determined according to the following procedures. Firstly, 10 mg of material were air-dried and weighed. Then, they were immersed in 15 mL of liquid medium solution for different time intervals. Wet samples were wiped with filter paper to remove excess liquid and weighed. The effect of salts on swelling behavior was evaluated by immersing a determined number of beads in NaCl, $CaCl_2$, and $MgCl_2$ aqueous solutions (0.15 mol/L). The swelling degree (SD) was calculated as (Equation (5)):

$$SD(\%) = \frac{W_w - W_{dry}}{W_{dry}} \times 100 \tag{5}$$

where W_w and W_{dry} are the weights of the beads measured at a specific time point and the initial weight of air-dried samples.

The release kinetics of capsaicin were performed by ultraviolet spectrometric measurement using a Spectrometer UV-2401 PC Shimadzu (Japan). A total of 200 mg of beads were placed into 10 mL of water and stirred at 100 rpm in an orbital shaker (VDRL MOD. 711+ Asal S.r.l.). The release medium was withdrawn at fixed time intervals before performing the UV-Vis analysis by analyzing the considered band at 281 nm. The experimental data were fitted according to Baker and Lonsdale model (Equation (6)) [26].

$$\frac{3}{2} \times \left\{ 1 - \left(1 - \frac{M_t}{M_\infty} \right)^{\frac{2}{3}} \right\} \times \frac{M_t}{M_\infty} = k \frac{t}{r^2} \tag{6}$$

where M_t is the amount of drug released at time t, M_∞ is the amount of drug released at infinite time, k is the Baker–Lonsdale release constant, and r is the radius bead, supposing it to have a spherical shape [27]. Since the beads underwent swelling phenomena, the bead radius is supposed to be time-dependent (r = r(t)).

Weed growth tests were performed as described hereafter. Petri dishes (Ø = 13 mm) were filled with commercial soil. *Cynodon dactylon* seeds were spread on the soil with a fixed ratio weight/surface (12 g/m^2). The rice milk-based beads were distributed on the soil (7.5 mg/mm^2). The Petri dishes were placed in an uncovered gazebo at ambient conditions (25 ± 5 °C and HR = 55 ± 3%). The soil was kept moist by sprinkling a certain amount of water (15 mL) three times a day. The test was conducted for 12 days.

2.5. Statistical Analysis

The statistical significance of the obtained data was assessed by performing a one-way ANOVA test. Tukey's post-hoc method was conducted for assessing significant differences between means ($p < 0.05$). The statistical comparisons were obtained by means of the Statistix 8.1 software (Analytical Software, Miller Landing Rd, Tallahassee, FL, USA).

3. Results

3.1. Chili Pepper Extract Composition

Capsacinoids are a complex mixture of several organic compounds. Prior to performing UV-Vis analysis, the PE composition was determined by conducting a UHPLC-MS analysis for the identification of the main compounds [28]. The spectrum is reported in Figure 2.
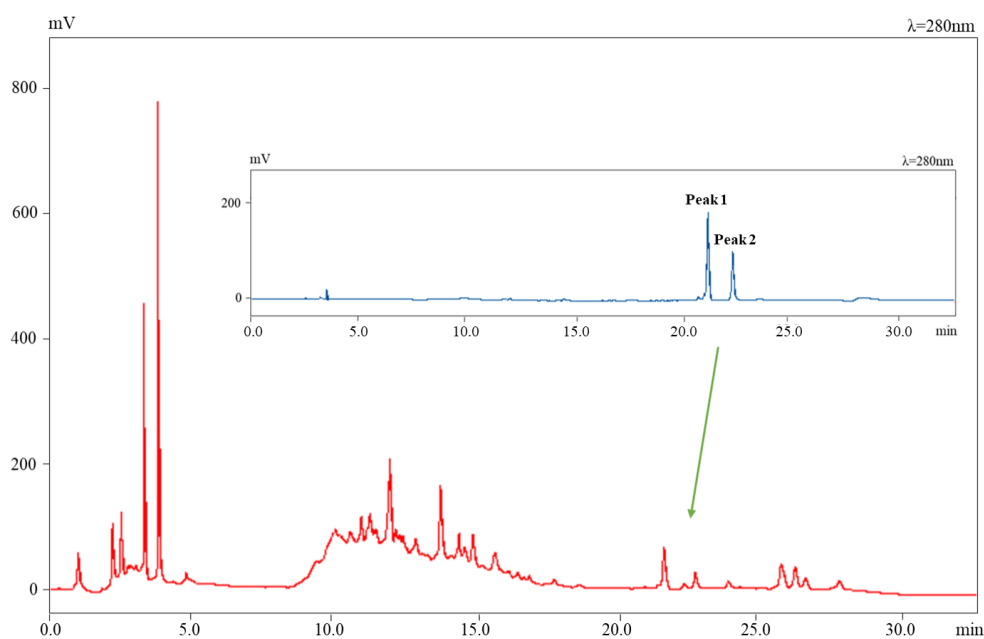

Figure 2. UHPLC-UV-Vis (λ = 280 nm) chromatographic profile of the extract (Peak 1: Capsaicin standard; Peak 2: Dihydrocapsaicin standard).

Table 1 reports the chemical formulas of the identified compounds.

Table 1. Chemical formulas and tentative identification of compounds.

Compound Name	t_R (min)	$[M - H]^+$ (*m/z*)	$[M - H]^-$ (*m/z*)	MS^2 (*m/z*)	Chemical Formula	Error (ppm)
Apigenin C-pentosyl-C-hexoside	10.97	-	563.1400	443.10 269.05	$C_{26}H_{27}O_{14}$	0.10
Capsaicin	15.92	306.2061	-	182.1540 132.0596	$C_{18}H_{27}O_3N$	−1.63
Dihydrocapsaicin	16.73	308.2216	-	184.1697 137.0596	$C_{18}H_{29}O_3N$	−1.99

t_R = retention time of LC-MS/MS spectra (Figure S2).

MS/MS spectra are reported as Figure S1 while TICs of chili pepper extract obtained by LC-MS analysis are reported in Figure S2.

3.2. Morphological Analysis of Beads

Figure 3 reports SEM micrographs of rice milk-based beads. From the SEM micrographs, it is evident the formation of a surface texture that is rough and uneven.
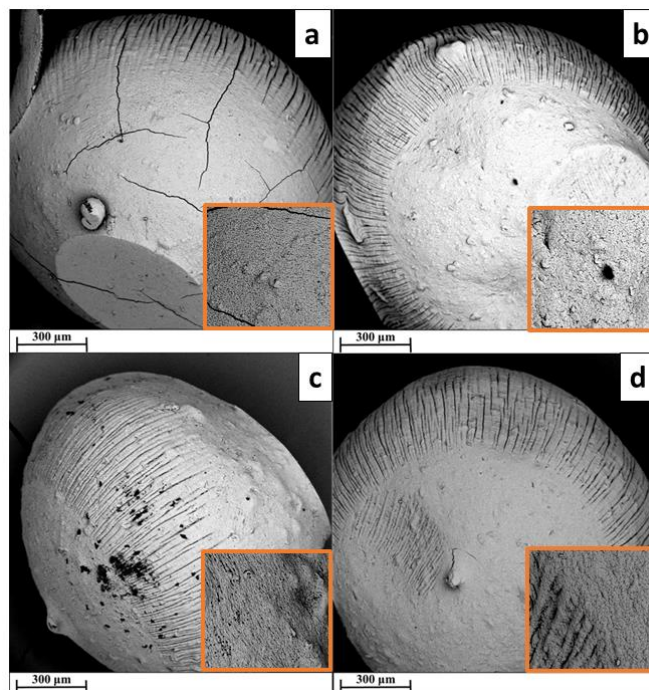

Figure 3. SEM micrographs of B-PE beads (**a**) B-PE-0, (**b**) B-PE-2.5; (**c**) B-PE-10 and (**d**) B-PE-20.

However, the surface morphology did not seem to change after the introduction of PE. The high-resolution images of the beads surface revealed that the sample is very rough with plenty of wrinkles and folds, a characteristic that could favor the diffusion of the encapsulated herbicide. EDX spectra of B-PE-20% (Figure 4) demonstrated the presence of capsaicinoids on the beads since the presence of nitrogen. Conversely, calcium and sodium can be associated with $CaCl_2$ and sodium alginate residues. The elemental mappings confirm that these elements are homogeneously distributed onto the surface.
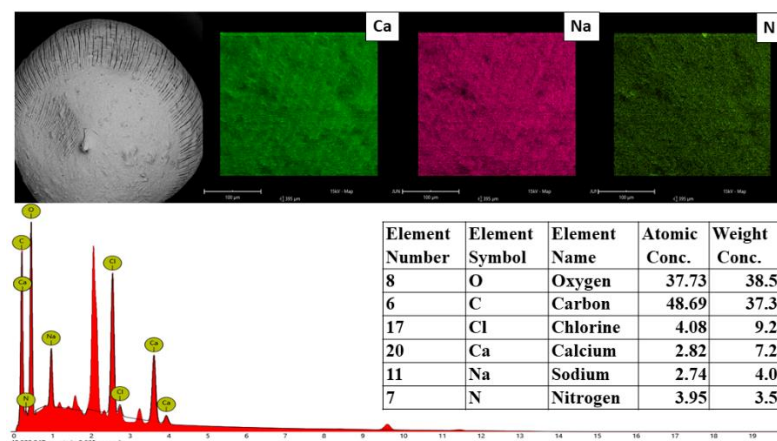

Element Number	Element Symbol	Element Name	Atomic Conc.	Weight Conc.
8	O	Oxygen	37.73	38.59
6	C	Carbon	48.69	37.38
17	Cl	Chlorine	4.08	9.24
20	Ca	Calcium	2.82	7.23
11	Na	Sodium	2.74	4.02
7	N	Nitrogen	3.95	3.54

Figure 4. EDX maps of B-PE-20%.

3.3. Swelling Degree Analysis

Figure 5 reports the normalized beads diameter (D(t)/D(t = 0)) for rice milk-based beads.
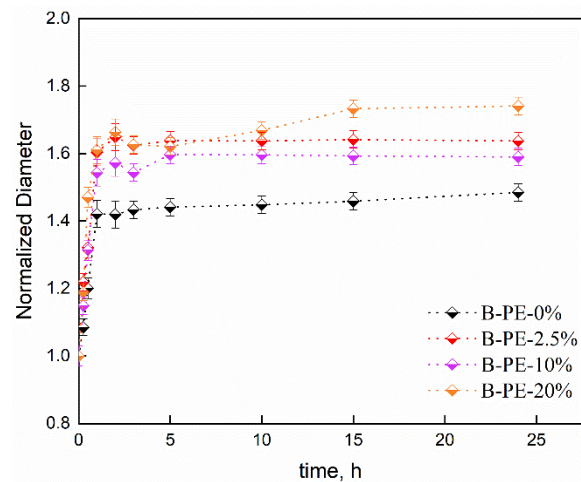

Figure 5. Normalized diameter trends over time as a function of PE content.

Figure 5 highlights the exponential increase in the beads' diameter over time. Compared to a neat rice milk bead, the presence of PE seems to favor the water adsorption and so the swelling of beads determines an increase in volume. No statistical difference was observed for B-PE-2.5% and B-PE-10% while a significant increase in mean diameter was observed for B-PE-20%, probably due to the hydrophilic nature of chili powder. The change of normalized diameter was modeled through Equation (7):

$$\frac{D}{D_0} = a + b \times \exp\left(-\frac{t}{c}\right) \tag{7}$$

where D_0 is the diameter at t = 0, a and b are constant to be determined; c is a time constant (h). As time approaches zero, the normalized diameter should be equal to 1 while as t tends to high values, D/D_0 approaches a maximum value of diameter (D_m). By modifying Equation (7), Equation (8) can be derived:

$$\frac{D}{D_0} = \frac{D_m}{D_0} + \left(1 - \frac{D_m}{D_0}\right) \times \exp\left(-\frac{t}{c}\right) \tag{8}$$

Table 2 reports the values extrapolated from the fitting process.

Table 2. Parameters of Equations (7) and (8).

Sample	a = D_m/D_0	b	c (h)	R^2
B-PE-0%	1.45 ± 0.016 [c]	−0.48 ± 0.02 [a]	0.66 ± 0.02 [a]	0.989
B-PE-2.5%	1.61 ± 0.013 [b]	−0.63 ± 0.03 [b]	0.57 ± 0.04 [b]	0.992
B-PE-10%	1.59 ± 0.015 [b]	−0.61 ± 0.03 [b]	0.58 ± 0.03 [b]	0.988
B-PE-20%	1.68 ± 0.022 [a]	−0.70 ± 0.03 [c]	0.49 ± 0.03 [c]	0.989

For each composite, different superscript letters in the same column indicate that the mean values are significantly different ($p \leq 0.05$).

After 24 h, the maximum diameter increases up to $1.45 \times D_0$, $1.61 \times D_0$, $1.59 \times D_0$, and $1.68 \times D_0$ for samples loaded with 0, 2.5, 10, and 20%, respectively. As Table 2 shows, there are no noticeable differences between samples loaded with 2.5 and 10% of PE, while a significant increase in bead diameter was observed for B-PE-20%. This was justified by the fact that the high hydrophilicity of PE could improve water adsorption since the exposure of a high number of polar sites. To better understand the effect of PE on an increase in

volume, a swelling test was conducted. Pictures of swelled beads, as a function of time, and swelling data were reported in Figure 6.
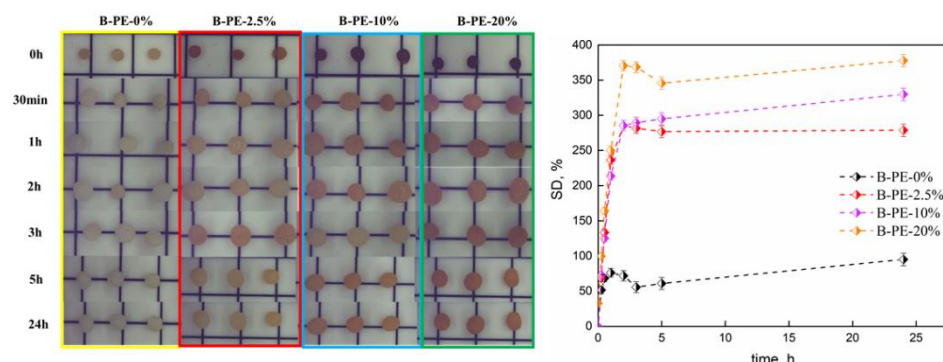

Figure 6. Pictures of swelled B-PE (**left**) and swelling degrees (%) of beads as a function of time at different PE content (**right**).

For short times, the rate of water uptake sharply increases and then levels off. The presence of hydrostatic repulsion between macromolecules is due to water molecules, which occupy a certain volume and led to an expansion of the structure [29]. Since that, it follows an increase of SD as PE content increases. The trends of SDs are perfectly in agreement with mean diameters variations, as previously reported, highlighting an evident difference between unloaded beads and PE-loaded rice milk-based beads. Figure 7 reports the swelling degrees of beads in presence of salt aqueous solutions.

As shown in Figure 7, the prepared beads adsorbed, except from NaCl solution, fewer amounts of water from saline solutions compared to distilled water. This is supposed to be caused by ionic hydrogels related to the screening effect of the metal cations. The presence of metal cations in the bulk media led to a decrease in the osmotic pressure difference between the hydrogel network and the external solution, so a lower amount of water was absorbed. In addition, the swelling capacity decreased with an increase in the charge of the cations (Mg^{2+} and Ca^{2+} possess a higher charge than monovalent cations like Na^+) since, as known, the porosity of hydrogels decreases as ionic strength increases since they are considered polyelectrolytes. In addition, Mg^{2+} and Ca^{2+} can chelate COO^- groups, leading to a compact network; conversely, the smaller the radius of atoms of some valent monoatomic cations, the more the water absorption capacity $Na^+ > Ca^{2+} > Mg^{2+}$ [30].
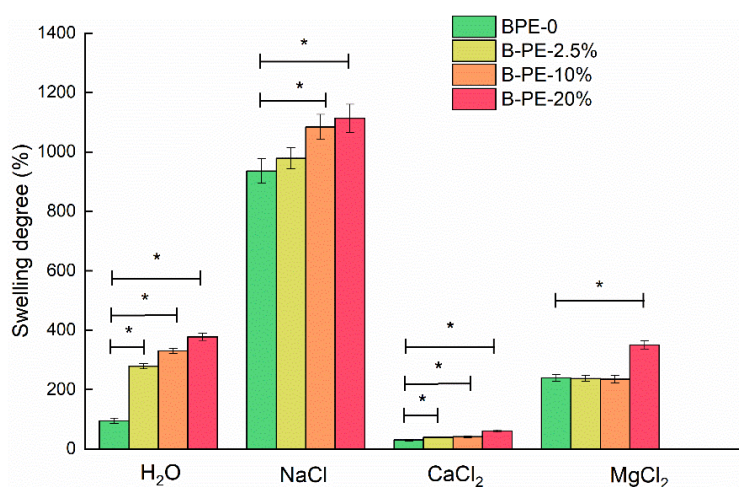

Figure 7. Swelling degrees of rice milk-based beads in salt aqueous solutions (* means that statistical differences are present between the samples).

3.4. Barrier Properties Evaluation

Figure 8 shows the sorption data of rice milk beads composites, reporting the equilibrium moisture content q_e (on a dry basis) as a function of the water concentration C_{eq} (g/L). The investigation of sorption properties is fundamental to understand the behavior of the produced delivery beads for outdoor exposures such as agricultural ones. The evaluation of barrier properties is crucial to the ability of the obtained composites to absorb and retain a determined amount of water.
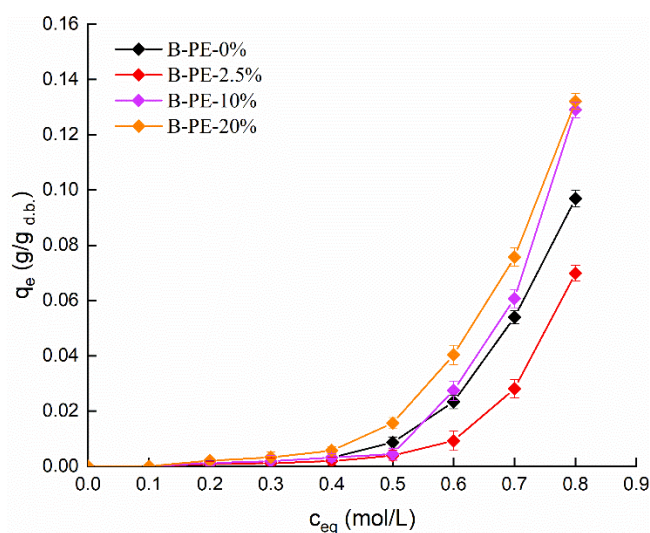

Figure 8. Sorption isotherms.

The sorption data show that for B-PE-2.5% a reduction of water content, especially at high activities, was observed probably due to the formation of an interconnected network between the polysaccharides of rice milk and the capsaicinoids functional groups. The improvement in sorption reduction is needed to avoid the probability of clustering occurring or the alteration of composite properties due to the formation of cracks induced by swelling and shrinkage phenomena. As PE content increases, an improvement in adsorbed water content was observed since the hydrophilic nature of the natural extract. So, a higher amount of water was absorbed by the bio-based beads. Sorption data have been fitted through four different models reported in the Section 2. The extrapolated parameters from Equations (1)–(4) are reported in Table 3. Plots representing sorption data fitted with the chosen isotherm models are reported in Supporting Information (Figure S3).

As proved by data reported in Table 3, Temkin and Freundlich models are not suitable since the coefficient of determination (R^2) is quite low. Langmuir model appeared to be not appropriate since the negative values of q_m, which is not acceptable. So, the polynomial model, despite the fact that its parameters do not have a precise physical meaning, is perfectly able to fit the sorption data. The sorption parameters can be evaluated considering Henry's law of solubility (Equation (9)):

$$S = \frac{dq_e}{dP} \tag{9}$$

The evaluation of the tangent to the fitting polynomial model for low equilibrium concentrations allowed to easily calculate the sorption parameter (Table 4).

Table 3. Parameters obtained by fitting experimental sorption data with the proposed models.

	B-PE-0%	B-PE-2.5%	B-PE-10%	B-PE-20%
	Polynomial model			
A_0	0	0	0	0
A_1	21.5	29.9	7.32	37.63
A_2	−101.7	347.2	86.8	−221.66
A_3	41.4	1053.1	−596.7	352.3
A_4	303.2	1002.3	910.6	155.2
R^2	0.998	0.995	0.998	0.999
	Langmuir model			
q_m (mg/g)	−2.85	−2.27	−4.16	−6.25
K_L (L/mg)	−875	−733.3	−750	−761.9
R^2	0.954	0.931	0.715	0.922
	Freundlich model			
K_F (L/mg)	0.01	0.01	0.02	0.03
n	0.42	0.38	0.43	0.42
R^2	0.851	0.832	0.821	0.781
	Temkin model			
RT/b (mg/g)	78.7	49.5	97.5	110.8
K_t (L/mg)	0.17	0.17	0.17	0.18
R^2	0.474	0.385	0.426	0.517

Table 4. Sorption coefficients were obtained from the polynomial model.

Sample	Sorption (g/g $_{d.b.}$ ×/atm)
B-PE-0%	0.72 ± 0.02 [b]
B-PE-2.5%	0.55 ± 0.01 [a]
B-PE-10%	1.17 ± 0.09 [c]
B-PE-20%	1.26 ± 0.04 [c]

For each composite, different superscript letters in the same column indicate that the mean values are significantly different ($p \leq 0.05$).

Proper interactions are supposed to occur between the sugars-based matrix and PE functional groups. Reduced water sorption of rice milk beads-2.5% can be a consequence of enhanced interaction of polysaccharides chains and OH groups that are less available for the interactions with water vapor.

3.5. Release Kinetic Evaluation

To test the capability of rice milk-based beads to be used as controlled release systems, we followed the release of the major component in the PE which could be detected by UV-Vis spectrophotometer, which is the capsaicin. Its release from polymeric composites was followed over time. The release of the encapsulated functional molecule is due to the entry of water molecules toward the bulk and thereby the counter diffusion movement of molecules to the external surface followed by its complete release. Figure 9 reports the release data of PE.
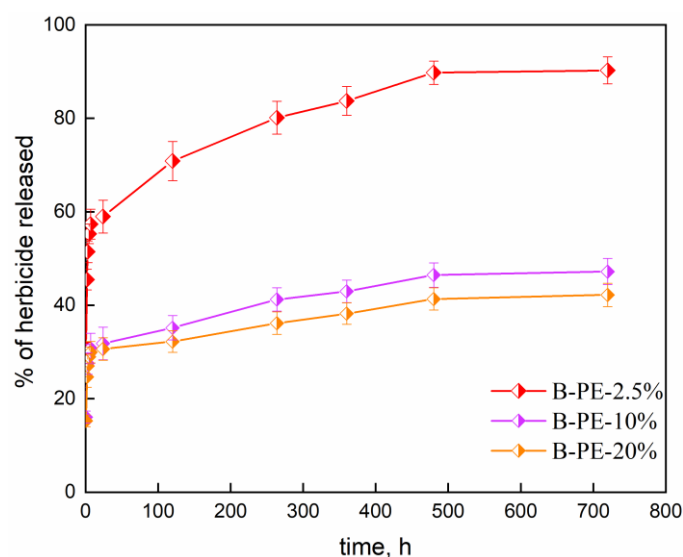
Figure 9. Release kinetics of Capsaicin.

The mechanism of drug releases is known to be due to many parameters (physical properties, drug-to-polymer ratio, geometric shape of matrix, and swelling phenomena) [31]. Figure 9 shows that the release rate of capsaicin is dependent on the loaded amount. The initial burst release is supposed to be related to the free functional compound. Moreover, the penetrating water molecules could generate phenomena such as relaxation of polymer chains and hydration [32]. The adsorbed water molecules could then enhance the internal pressure allowing the herbicide to be released and promoting the burst release effect. Moreover, it is worth noting that the burst is reduced as the PE amount increases, as consequence of the higher stability of the polymeric bead network which likely is able to form hydrogen bonds with PE. Then, a slower and more controlled release was detected [33]. As shown in Figure 9, after 10 days more than 80% of PE is released. Moreover, 41% and 36% of PE are released after 10 days for B-PE-10% and B-PE-20%, respectively. At a low PE amount, the SD is reduced, as previously reported. As the PE amount increases, the B-PE structure is more stable, and the beads are able to better adsorb water molecules determining an increase in SD. The adsorption of a high amount of water and the increasing of gel volume could act as a barrier for the counter diffusion of capsaicin; it could slow down the release rate justifying the lower amount of capsaicin released. Probably, water molecules act as a physical barrier, which improves the mass transfer resistance by increasing the tortuosity of the system. By applying a modified Baker and Lonsdale model, substituting Equation (7) into Equation (6), it was possible to derive Equation (10):

$$\frac{3}{2} \times \left\{ 1 - \left(1 - \frac{M_t}{M_\infty} \right)^{\frac{2}{3}} \right\} \times \frac{M_t}{M_\infty} = 4 \times k \frac{t}{\left[D_0 \times \left(a + b \times \exp\left(-\frac{t}{c} \right) \right) \right]^2} \tag{10}$$

The fitting process of release kinetic curves allowed to obtain the k parameter which is reported in Table 5:

Table 5. k parameters obtained from fitting of experimental data applying Equation (10).

Sample	k (mm^2 × h^{-1})
B-PE-2.5%	0.0053 ± 0.0008 [a]
B-PE-10%	0.0031 ± 0.0006 [b]
B-PE-20%	0.0022 ± 0.0009 [b]

For each composite, different superscript letters in the same column indicate that the mean values are significantly different ($p \leq 0.05$).

The fitting of experimental release data by applying Equation (10) allows us to evaluate the release constants (k) to support the previous reported statements. The k diffusion constant underwent a decrease as PE content increased, which could be attributed to the different swelling behavior of fabricated beads. Since the k constant could be considered directly proportional to the diffusion coefficient, its reduction increases may be related to the increase in mass transfer resistance, allowing to tune the release profile of an encapsulated herbicide without spreading it in a short time. Finally, it could be claimed that a novel agricultural compound delivery system, completely based on renewable resources, has been designed to achieve controlled release. It is worthwhile claiming that the release system, made of aqueous rice milk-PE material solution, is completely sustainable; no other similar systems have been reported.

3.6. In Vivo Tests: Effect of PE Loaded Beads against Cynodon dactylon Growth

Figure 10 shows the in vivo tests performed as previously described. Each Petri dish contains a determined amount of seeds and beads, dispersed on the soil and watered periodically.
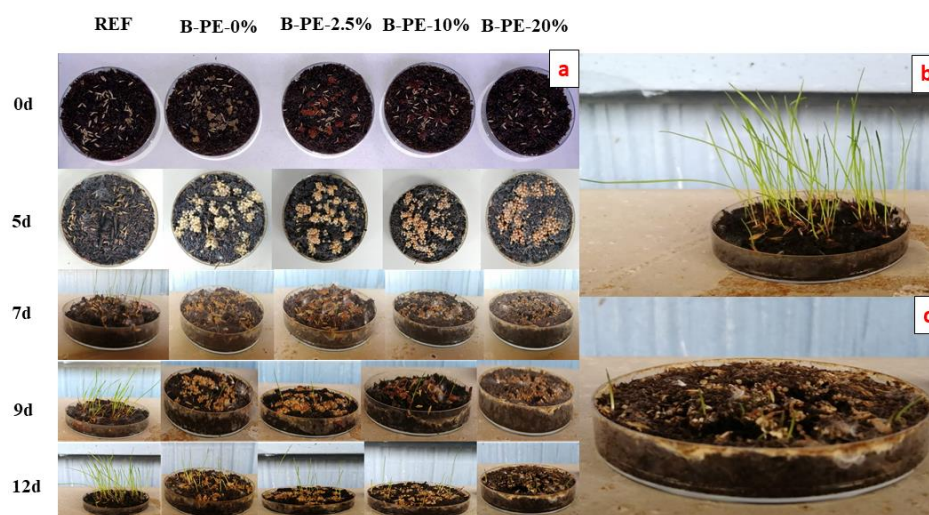

Figure 10. (**a**) Weeds growth over time; (**b**) effect of B-PE-0%; and (**c**) B-PE-20% on weeds growth after 12 days.

Figure 10 highlights that seeds were germinated and grown in absence of capsaicinoids; while in presence of an increasing concentration of chili pepper extract, the growth of weeds is noticeably reduced and slowed down. The length of weeds in presence of neat soil roughly reached 12 cm while the length is clearly shorter as the PE content increases.

There was no significant difference in growth rate of weed seeds in presence of B-PE-2.5% and BPE-10% while a quasi-total blocking of weed growth was observed for weeds in contact with BPE-20% (Figure 10c). As shown, the weeds in contact with herbicide delivery sustained beads were strongly arrested proving that the sustained-release system had an effective herbicidal ability, whereas the weeding time would be prolonged due to the slow release of PE for highly loaded beads. The results suggest that the PE had positive response with respect to the blocking or slowing down of weeds proliferation.

4. Conclusions

In this study, composites based on rice milk, using alginate as a forming agent, were produced through gelation in $CaCl_2$ solution. Chili pepper extract was extracted from chili peppers through a water/EtOH solution and used as a potential green herbicide. SEM micrographs evidence the roughness and the presence of pores and cracks on the beads surface. Barrier properties resulted dependent on PE concentration which hydrophilicity noticeably increased the adsorbed water content. Swelling phenomena were studied over time (up to 24 h) and demonstrated a different behavior of beads varying the PE content

and the ionic strength. The release kinetics of capsaicin appeared to be dependent on PE content. In particular, after an initial burst, the release seems to be slowed down as PE content increases, probably due to the formation of an interconnected network stabilized by hydrogen bonds, which makes a physical hindrance for the counter diffusion of capsaicin. Finally, in vivo tests were conducted using *Cynodon dactylon* as studied weed. The results showed a noticeable slowing down of weed growth when the soil was covered with B-PE-2.5% and a quasi-complete inhibition of weed growth after 12 days when the soil was covered with B-PE-20%. The results demonstrated the possibility of tailoring the release of a loaded compound by designing natural polymeric devices through an environmentally friendly methodology. A phytotoxicity test will be conducted to further support the performances of the produced systems.

References

1. Zeng, X.; Zhong, B.; Jia, Z.; Zhang, Q.; Chen, Y.; Jia, D. Halloysite Nanotubes as Nanocarriers for Plant Herbicide and Its Controlled Release in Biodegradable Polymers Composite Film. *Appl. Clay Sci.* **2019**, *171*, 20–28. [CrossRef]
2. Essandoh, M.; Wolgemuth, D.; Pittman, C.U.; Mohan, D.; Mlsna, T. Phenoxy Herbicide Removal from Aqueous Solutions Using Fast Pyrolysis Switchgrass Biochar. *Chemosphere* **2017**, *174*, 49–57. [CrossRef]
3. Yang, W.; Zhou, M.; Oturan, N.; Li, Y.; Su, P.; Oturan, M.A. Enhanced Activation of Hydrogen Peroxide Using Nitrogen Doped Graphene for Effective Removal of Herbicide 2,4-D from Water by Iron-Free Electrochemical Advanced Oxidation. *Electrochim. Acta* **2019**, *297*, 582–592. [CrossRef]
4. Huang, X.; Feng, S.; Zhu, G.; Zheng, W.; Shao, C.; Zhou, N.; Meng, Q. Removal of Organic Herbicides from Aqueous Solution by Ionic Liquid Modified Chitosan/Metal-Organic Framework Composite. *Int. J. Biol. Macromol.* **2020**, *149*, 882–892. [CrossRef]
5. Wang, S.; Jia, Z.; Zhou, X.; Zhou, D.; Chen, M.; Xie, D.; Luo, Y.; Jia, D. Preparation of a Biodegradable Poly(Vinyl Alcohol)–Starch Composite Film and Its Application in Pesticide Controlled Release. *J. Appl. Polym. Sci.* **2017**, *134*, 45051. [CrossRef]
6. Mfarrej, M.F.B.; Rara, F.M. Competitive, Sustainable Natural Pesticides. *Acta Ecol. Sin.* **2019**, *39*, 145–151. [CrossRef]
7. Yang, R.; Xu, T.; Fan, J.; Zhang, Q.; Ding, M.; Huang, M.; Deng, L.; Lu, Y.; Guo, Y. Natural Products-Based Pesticides: Design, Synthesis and Pesticidal Activities of Novel Fraxinellone Derivatives Containing N-Phenylpyrazole Moiety. *Ind. Crops Prod.* **2018**, *117*, 50–57. [CrossRef]
8. Copping, L.G.; Menn, J.J. Biopesticides: A Review of Their Action, Applications and Efficacy. *Pest Manag. Sci.* **2000**, *56*, 651–676. [CrossRef]
9. Roy, A.; Singh, S.; Bajpai, J.; Bajpai, A. Controlled Pesticide Release from Biodegradable Polymers. *Cent. Eur. J. Chem.* **2014**, *12*, 453–469. [CrossRef]
10. Wang, C.; Ye, W.; Zheng, Y.; Liu, X.; Tong, Z. Fabrication of Drug-Loaded Biodegradable Microcapsules for Controlled Release by Combination of Solvent Evaporation and Layer-by-Layer Self-Assembly. *Int. J. Pharm.* **2007**, *338*, 165–173. [CrossRef] [PubMed]

11. Selina, O.E.; Chinarev, A.A.; Obukhova, P.S.; Bartkowiak, A.; Bovin, N.V.; Markvicheva, E.A. Alginate-Chitosan Microspheres for the Specific Sorption of Antibodies. *Russ. J. Bioorganic Chem.* **2008**, *34*, 468–474. [CrossRef]
12. Panos, I.; Acosta, N.; Heras, A. New Drug Delivery Systems Based on Chitosan. *Curr. Drug Discov. Technol.* **2008**, *5*, 333–341. [CrossRef]
13. Chang, C.P.; Leung, T.K.; Lin, S.M.; Hsu, C.C. Release Properties on Gelatin-Gum Arabic Microcapsules Containing Camphor Oil with Added Polystyrene. *Colloids Surf. B Biointerfaces* **2006**, *50*, 136–140. [CrossRef]
14. Ismail Abou-Dobara, M.; Mohamed Ismail, M.; Mohamed Refaat, N. Chemical Composition, Sensory Evaluation and Starter Activity in Cow, Soy, Peanut and Rice Milk. *J. Nutr. Health Food Eng.* **2016**, *5*, 1–8. [CrossRef]
15. FoodData Central. Available online: https://fdc.nal.usda.gov/fdc-app.html#/food-details/171942/nutrients (accessed on 15 June 2022).
16. Zhang, S.; Wei, F.; Han, X. An Edible Film of Sodium Alginate/Pullulan Incorporated with Capsaicin. *New J. Chem.* **2018**, *42*, 17756–17761. [CrossRef]
17. Zhao, J.; Wei, F.; Xu, W.; Han, X. Enhanced Antibacterial Performance of Gelatin/Chitosan Film Containing Capsaicin Loaded MOFs for Food Packaging. *Appl. Surf. Sci.* **2020**, *510*, 145418. [CrossRef]
18. Srithar, S.; Rao, S.S. Capsicum-Extract Blended Chitosan Composite Films and Studying Their Antibacterial Properties. *Bull. Mater. Sci* **2019**, *42*, 149. [CrossRef]
19. Viscusi, G.; Gorrasi, G. Gelatin Beads/Hemp Hurd as PH Sensitive Devices for Delivery of Eugenol as Green Pesticide. *J. Polym. Environ.* **2021**, *29*, 3756–3769. [CrossRef]
20. Viscusi, G.; Lamberti, E.; Gorrasi, G. Design of Sodium Alginate/Soybean Extract Beads Loaded with Hemp Hurd and Halloysite as Novel and Sustainable Systems for Methylene Blue Adsorption. *Polym. Eng. Sci.* **2021**, *62*, 129–144. [CrossRef]
21. Viscusi, G.; Lamberti, E.; Gorrasi, G. Design of a Hybrid Bio-Adsorbent Based on Sodium Alginate/Halloysite/Hemp Hurd for Methylene Blue Dye Removal: Kinetic Studies and Mathematical Modeling. *Colloids Surfaces A Physicochem. Eng. Asp.* **2022**, *633*, 127925. [CrossRef]
22. Kelebek, H.; Sevindik, O.; Uzlasir, T.; Selli, S. LC-DAD/ESI MS/MS Characterization of Fresh and Cooked Capia and Aleppo Red Peppers (*Capsicum annuum* L.) Phenolic Profiles. *Eur. Food Res. Technol.* **2020**, *246*, 1971–1980. [CrossRef]
23. Elanchezhiyan, S.S.; Preethi, J.; Rathinam, K.; Njaramba, L.K.; Park, C.M. Synthesis of Magnetic Chitosan Biopolymeric Spheres and Their Adsorption Performances for PFOA and PFOS from Aqueous Environment. *Carbohydr. Polym.* **2021**, *267*, 118165. [CrossRef]
24. Golie, W.M.; Upadhyayula, S. An Investigation on Biosorption of Nitrate from Water by Chitosan Based Organic-Inorganic Hybrid Biocomposites. *Int. J. Biol. Macromol.* **2017**, *97*, 489–502. [CrossRef]
25. Hasan, M.; Ahmad, A.L.; Hameed, B.H. Adsorption of Reactive Dye onto Cross-Linked Chitosan/Oil Palm Ash Composite Beads. *Chem. Eng. J.* **2008**, *136*, 164–172. [CrossRef]
26. Rani, S.; Sharma, A.K.; Khan, I.; Gothwal, A.; Chaudhary, S.; Gupta, U. Polymeric Nanoparticles in Targeting and Delivery of Drugs. In *Nanotechnology-Based Approaches for Targeting and Delivery of Drugs and Genes*; Elsevier Inc.: Amsterdam, The Netherlands, 2017; pp. 223–255. ISBN 9780128097182.
27. Chien, Y.W. Controlled Release of Biologically Active Agents. *J. Pharm. Sci.* **1988**, *77*, 371. [CrossRef]
28. Abate, M.; Pepe, G.; Randino, R.; Pisanti, S.; Basilicata, M.G.; Covelli, V.; Bifulco, M.; Cabri, W.; D'ursi, A.M.; Campiglia, P.; et al. Ganoderma Lucidum Ethanol Extracts Enhance Re-Epithelialization and Prevent Keratinocytes from Free-Radical Injury. *Pharmaceuticals* **2020**, *13*, 224. [CrossRef]
29. Martínez-Ruvalcaba, A.; Becerra-Bracamontes, F.; Sánchez-Díaz, J.C.; González-Álvarez, A. Polyacrylamide-Gelatin Polymeric Networks: Effect of PH and Gelatin Concentration on the Swelling Kinetics and Mechanical Properties. *Polym. Bull.* **2009**, *62*, 539–548. [CrossRef]
30. Shivakumara, L.R.; Demappa, T. Synthesis and Swelling Behavior of Sodium Alginate/Poly(Vinyl Alcohol) Hydrogels. *Turkish J. Pharm. Sci.* **2019**, *16*, 252. [CrossRef]
31. Ainurofiq, A.; Choiri, S. Drug Release Model and Kinetics of Natural Polymers-Based Sustained Release Tablet. *Lat. Am. J. Pharm.* **2015**, *37*, 1328–1337.
32. Ford, J.L.; Rubinstein, M.H.; McCaul, F.; Hogan, J.E.; Edgar, P.J. Importance of Drug Type, Tablet Shape and Added Diluents on Drug Release Kinetics from Hydroxypropylmethylcellulose Matrix Tablets. *Int. J. Pharm.* **1987**, *40*, 223–234. [CrossRef]
33. Gallagher, K.M.; Corrigan, O.I. Mechanistic Aspects of the Release of Levamisole Hydrochloride from Biodegradable Polymers. *J. Control. Release* **2000**, *69*, 261–272. [CrossRef]